Steel and Composite Structures, *Vol. 32, No. 1* (*2019*) *79-90*
DOI: https://doi.org/10.12989/scs.2019.32.1.079

Experimental evaluation of steel connections with horizontal slit dampers

Hossein Akbari Lor, Mohsen Izadinia* and Parham Memarzadeh

Department of Civil Engineering, Najafabad Branch, Islamic Azad University, Najafabad, Iran

(*Received July 31, 2018, Revised May 2, 2019, Accepted May 31, 2019*)

Abstract. This study introduces new connections that connect the beam to the column with slit dampers. Plastic deformations and damages concentrate on slit dampers. The slit dampers prevent plastic damages of column, beam, welds and panel zone and act as fuses. The slit dampers were prepared with IPE profiles that had some holes in the webs. In this paper, two experimental specimens were made. In first specimen (SDC1), just one slit damper connected the beam to the column and one IPE profile with no holes connected the bottom flange of the beam to the column. The second specimen (SDC2) had two similar dampers which connected the top and bottom flange of the beam to the column. Cyclic loading was applied on Specimens. The cyclic displacements conditions continued until 0.06 radian rotation of connection. The experimental observations showed that the bending moment of specimen SDC2 increased until 0.04 story drift. In specimen SDC1, the bending moment decreases after 0.03 story drift. Test results indicate the high performance of the proposed connection. Based on the results, the specimen with two slit damper (SDC2) has higher seismic performance and dissipates more energy in loading process than specimen SDC1. Theoretical formulas were extended for the proposed connections. Numerical studies have been done by ABAQUS software. The theoretical and numerical results had good agreements with the experimental data. Based on the experimental and numerical investigations, the high ductility of connection is obtained from plastic damages of slit dampers. The most flexural moment of specimen SDC1 occurred at 3% story drift and this value was 1.4 times the plastic moment of the beam section. This parameter for SDC2 was 1.73 times the plastic moment of the beam section and occurred at 4% story drift. The dissipated energy ratio of SDC2 to SDC1 is equal to 1.51.

Keywords: slit damper; steel connection; moment capacity; energy dissipation; ductility; cyclic loading

1. Introduction

An aim of the seismic design is the increase of structure ductility. Use of hysteretic dampers in structures can increase ductility and dissipation of seismic energy. Some dampers dissipate energy due to plastic deformations and damages. These dampers yield because of bending moments, torques, axial forces or shear forces.

Northridge earthquake caused failure in some steel buildings in 1994. Steel connections experienced the most damages during the earthquake. Before the Northridge earthquake, the low ductility of common steel connections had been proved by some experimental studies by Popov and Tsai (1989). Ductile connections are able to increase plastic rotation and moment capacity of the connections. After the Northridge earthquake, the reduction of the beam section was investigated as a method which increases connections ductility (Jones *et al*. 2002). The Reduced Beam Section (RBS) connection is a practical connection in recent years. Based on the weakening idea, RBS connections are extended. In the weakening concept, the bending moment capacity of the beam is decreased near the column side. The beam section reduction is caused that damages concentrate on the plastic hinge. Plastic deformations are formed in the reduced part. The concentration of damage in the plastic hinge prevents failure of the welds so the plastic rotation capacity of the connection is increased. Tabar and Deylami (2006) studied major parameters affecting the instability of beam with RBS moment connection. The instability of the RBS beam always occurs after the plastic deformations. Reduction of the beam section was done by cutting some parts of flanges. Pachoumis *et al*. (2010) studied the cyclic performance of the RBS connections. They used experimental analysis and finite element models to simulate the connections. Also, the web reduction was investigated. Li *et al*. (2011) investigated the behavior of connections with an opening in the beam web. Mirghaderi *et al*. (2010) introduced a new reduction in the web that was named accordion web RBS connection. In this type of connection, the flat web of the beam is replaced by corrugated plates. These plates are located where it is expected that the plastic hinge forms. Saleh *et al*. (2016) studied on tubular web RBS connection. In this connection, the flat web of the beam is replaced by a tube. The tube is placed where it is expected plastic hinge forms. Also, Zahrai *et al*. (2017) studied this kind of connection and compared numerical and experimental results together. Karamodin and Zanganeh (2017) extended a new manner to estimate the plastic deformation capacity of structures elements. Farrokhi *et al*. (2010) studied the effects of structural detailing on seismic response of moment resisting connections in steel frames. Study on dampers more developed after the Northridge earthquake.

*Corresponding author, Ph.D.,
E-mail: izadinia@iaun.ac.ir

ISSN: 1229-9367 (Print), 1598-6233 (Online)

Zhou and Lu (2004) used a shaking table experiment on a three-story steel frame with metallic yield and oil dampers. They investigated the dynamic specifications and seismic energy dissipation performance of the system. Chan and Albermani (2008) theoretically and experimentally studied on slit dampers and presented some relations about the capacity of slit dampers. Metal dampers with different shapes were investigated and applied in buildings (Benavent-Climent 2010). The slit dampers are proper devices to dissipate seismic energy and could be used as devices of passive control in structures. In this type of control, structures are equipped with devices that do not need an exterior source of energy. Dampers and isolators were used as passive control devices of structures (Ibrahim 2008). Karavasilis *et al*. (2012) studied an alternative seismic design method for steel structures that concentrates damage in steel energy dissipation devices such as slit dampers and protects the main structural elements from yielding. Slit dampers were used in shear panels and steel shear walls recently. Ke and Chen (2014) developed a practical design and assessment approach of steel frames with steel slit walls. Hedayat (2015) investigated analytically and numerically on steel slit dampers and Finite element results were used to define the behavior of slit dampers. Several theoretical equations were proposed to predict the behavior of unbuckled steel slit dampers. Zheng *et al*. (2015) proposed a new steel damper with non-uniform vertical slits. They studied buckling resistance capacity and energy dissipation of this damper. He *et al*. (2016) studied the behavior of slit shear walls made of low yield point steel. These walls dissipated energy at small lateral drifts. Lu *et al*. (2016) studied steel plate shear walls with non-uniform spacing slits. Khatamirad and Shariatmadar (2017) investigated a slit shear wall which had vertical slits under lateral loads. The numerical and analytical analysis was done to study the effect of slit shape and edge stiffener on the behavior of steel slit shear wall. Kim *et al*. (2017) studied a seismic retrofit method for a structure using steel plate slit dampers. Amiri *et al*. (2018) studied the behavior of block slit damper device and theoretical, FE and experimental analyses were used. They also investigated stress and strain concentration and out of plane buckling in the slit dampers. Tagawa *et al*. (2016) experimentally studied frames with the passive vibration control system and steel slit dampers were used. Lateral stiffness and strength formula of the frame with this system were derived.

Lee and Kim (2015) investigated the seismic energy absorption of a hybrid damper which is made of a friction and a slit damper. Also, the seismic performance of the structure with hybrid damper was analyzed. Eldin *et al*. (2018) studied the seismic behavior of a hybrid damper made of a steel slit plate and friction pads. Shahri and Mousavi (2018) investigated connections with elliptic slit dampers. They studied the effects of dampers geometric parameters.

Use of metal dampers in the beam to column connections was studied recently. Dampers could be used in the beam flanges. Also, dampers could be placed in the beam web. Vasdravellis *et al*. (2012) proposed a steel post-tensioned connection with steel energy dissipation devices. Energy dissipation elements include steel cylindrical pins with an hourglass shape. The proposed elements are placed between the top and the bottom flanges of the beam. Mahjoubi and Maleki (2016) proposed a dual pipe damper and used it to connect the beam to the column. Seismic performance of steel frames with dual-pipe dampers was studied by them and design guidelines of structural control were suggested. Oh *et al*. (2009) proposed a new connection with slit damper which showed a good performance in experimental studies and all damages were absorbed by the slit dampers. Beams, columns and panel zones remained in the elastic state. In this structural system, the connection was equipped with a metallic damper. Plastic deformations were limited to the vertical slit dampers at the bottom flange of the beam. The seismic performance of the proposed connection was verified through cyclic tests of three full-scale steel structures that had slit dampers. This type of connection is shown in Fig. 1(a). Saffari *et al*. (2013) numerically and theoretically studied the use of slit dampers in the beam to column connections and proposed some new details. They added slit dampers at the top and bottom beam flanges to improve the connection behavior. These dampers are able to absorb and dissipate a significant amount of energy. Slit dampers caused a remarkable reduction in the plastic strain at the column face area and consequently kept plastic hinge formation away from the column face. One of the connection details which was proposed by them is shown in Fig. 1(b).

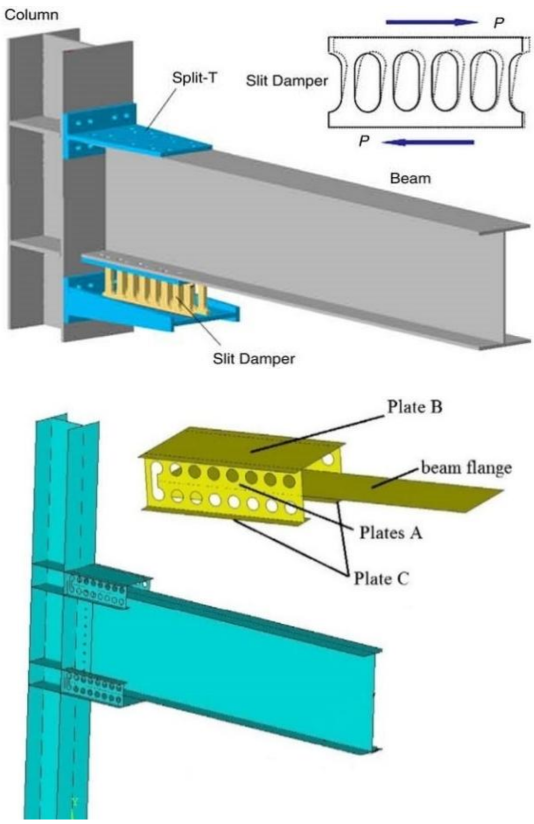

Fig. 1 Connections with vertical slit dampers
(a) Proposed by Oh *et al*. (2009);
(b) Proposed by Safari *et al*. (2013)

Most researchers who were mentioned above were intended to enhance the energy dissipation capacity of the structures. Some studies focused on connection ductility to dissipate more energy and prevent failure in the connections. This aim could be achieved by adding slit dampers to the connections. The present research intends to use horizontal slit dampers for passive control of the structure. It can be used as an energy dissipation device to increase the ductility of the proposed connections. Vertical slit dampers which were proposed by researchers may experience buckling in some loading cases due to compression forces but the horizontal slit dampers do not experience buckling in more loading cases. In this paper, two kinds of connections with the horizontal slit dampers are proposed. In the connections, I-shape slit dampers connect the beam to the column. Experimental, theoretical and numerical researches on the proposed connections have been investigated. Numerical studies have been done by ABAQUS software. Seismic behavior and strength of connections have been studied. The proposed connections increase ductility and bending moment capacity of the connection.

2. Proposed connections

In this study, proposed slit damper is an I-shape profile with rectangular slits in the web which have round corners. These slits are created in two rows in the web of the damper. The beam flange is connected to the slit damper web. End of slit dampers is connected to the column (Fig. 2). In this study, two experimental specimens were made. The main difference of two specimens is numbers of slit dampers in each specimen. First specimen (SDC1) had just one slit damper which was used at the top of the beam and connected the beam to the column and an I-shape profile without any slit connected the bottom beam flange to the column (Fig. 2(a)). In the second specimen (SDC2), two identical slit dampers connected the beam flanges to the column (Fig. 2(b)). These dampers transferred tension and compression forces to the column in seismic loading. This couple of forces provided a bending moment at the end of the beam. In the proposed connections, no part of the beam section welds to the column flange directly. Slits in dampers caused stress concentration in damper and yielding of steel materials. This matter dissipated seismic energy. Dissipation of energy by slit dampers increased the connection ductility. Because of steel materials yielding, inelastic rotation capacity of the connection was increased. One of the main parameters that specify the connection performance in the seismic loading is inelastic rotation capacity. According to seismic design codes criteria (AISC 341-10 2010, AISC 358-10 2010, FEMA-355D 2000 and FEMA-350 2000), inelastic rotation capacity of the connection must be at least 0.04 radian in special moment frames. Also, the minimum bending moment for 0.04 radian rotation must be at least $0.8M_p$ where M_p is the plastic moment of the beam. When the slit dampers are used, moment capacity is governed by the capacity of the slit dampers instead of the beam moment capacity. In this study, size of dampers and slits are designed in the way that

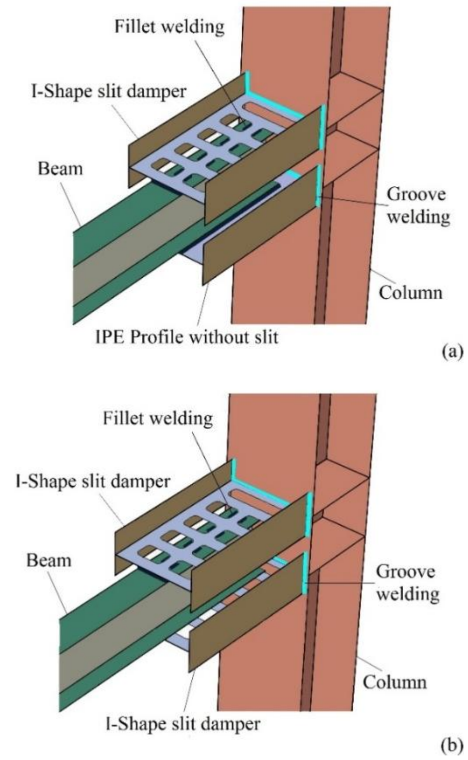

Fig. 2 Proposed connections: (a) Connection with one slit damper; (b) Connection with two slit dampers

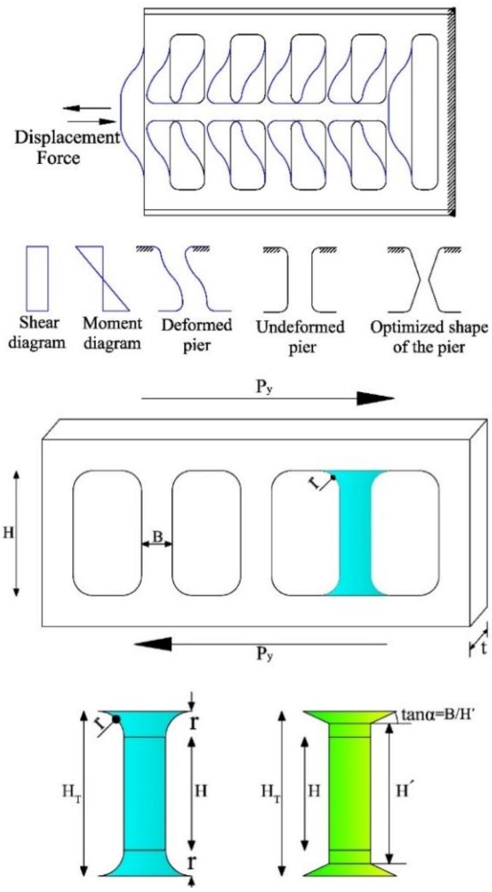

Fig. 3 Proposed slit damper: (a) Slit damper deformations, shear and moment diagram, and optimized shape of a pier; (b) One row of slit damper geometry

dampers materials yield before the beam materials. When piers of slit dampers yield, cracks and stresses are concentrated on the slit dampers and other parts of connection remain safe.

The shape of slits, arrangement and welding of slit dampers to the beams were designed to permit some parts of slit damper could have relative displacement parallel to the beam axis. This freedom of movement yields some parts of damper under seismic loading and dissipates some of the energy. A wide slit near the connection was made in the damper web. It causes the slit damper has freedom of movement. Deformations and relative movement freedom of a slit damper are shown in Fig. 3(a). Also, the bending moment and shear force diagrams for a strut of slit damper are shown in Fig. 3(a). As Fig. 3(a) shows, the maximum bending moments occur at the ends of the strut and cause stress concentration at these locations. According to the experimental results, cracks and failures were observed in the same places. Also, based on the numerical models, stress concentrations occurred at the ends of struts. The column, panel zone, and beam remained safe because of plastic deformation on the slit dampers. In practical projects, concrete slabs are existed and cover the top flange of the beams. In this case, upper slit damper must be covered by a secondary device such as a thin plate that prevents concrete to fill the slits. This issue caused upper slit damper acts in the way that it was designed.

3. Design of slit damper connections

In specimen SDC1, just one slit damper was used to connect the top flange of beam to the column. In specimen SDC2, two slit dampers connected the beam to the column. In each slit damper, two rows of slits existed. Fig. 3(b) shows one row of the struts and in-plane shear forces. According to previous researches (Chan and Albermani 2008 and Oh *et al*. 2009), two different mechanisms (Flexural yielding or shear yielding) could happen in the slit damper. If some simplifications are considered, yield strength (P_y) and ultimate strength (P_u) of just one struts row can be calculated as follows

$$P_y = min\left\{n\frac{\sigma_y.t.B^2}{2H'}, n\frac{2\sigma_y.t.B^2}{3\sqrt{3}}\right\} \tag{1}$$

$$P_u = min\left\{n\frac{\sigma_u.t.B^2}{2H'}, n\frac{2\sigma_u.t.B^2}{3\sqrt{3}}\right\} \tag{2}$$

In Eqs. (1) and (2), the first term is related to flexural moment and the second term is related to shear force.

Where n = number of struts; B = struts width; σ_y = yield stress; σ_u = ultimate stress; t = strut thickness and H' is the equivalent height of struts that is shown in Fig. 3(b). Oh *et al*. (2009) proposed H' as below

$$H' = H + \frac{2r^2}{H_T} \tag{3}$$

That H and H_T are shown in Fig. 3(b).

Because of stress concentration in the dampers, plastic deformations occur in the slit dampers struts. In the proposed connection, the bending moment of the beam is transferred to the column by a couple of forces.

Simplified models of the connections are shown in Fig. 4. Oh *et al*. (2009) proposed a similar analytical model for their slit damper connection. They assumed a rotational center for the connection and calculated the bending moment according to the distance between this point and damper forces.

In this study, two analytical models are introduced. In model 1, the beam is connected to the column by two springs. In fact, the I-shape profiles at the top and bottom flanges of the beam are modeled as springs. In this model, the center of rotation could be assumed a point on the axis of the beam as it is shown in Fig. 4. This model predicts the results close to the experimental and numerical data for specimen SDC2. But this model predicts the maximum bending moment of specimen SDC1 lower than the experimental and numerical data. The reason for this discrepancy is the differences between stiffness and structural properties of the upper and lower I-shape profiles (springs) in SDC1. This matter causes complicated load and stress distribution. Also, it changes the location of the rotation center. In specimen SDC1, the lower I-shape profile has no slits and has high rigidity and stiffness in comparison with the upper slit damper. Model 2 was introduced to predict the behavior of this specimen as it is shown in Fig. 4(b). In this model, it is assumed that the center of rotation is the lowest point of the bottom I-shape profile. Obtained results from model 2 are close to the experimental and numerical data of specimen SDC1.

Shear forces and bending moments of the connections

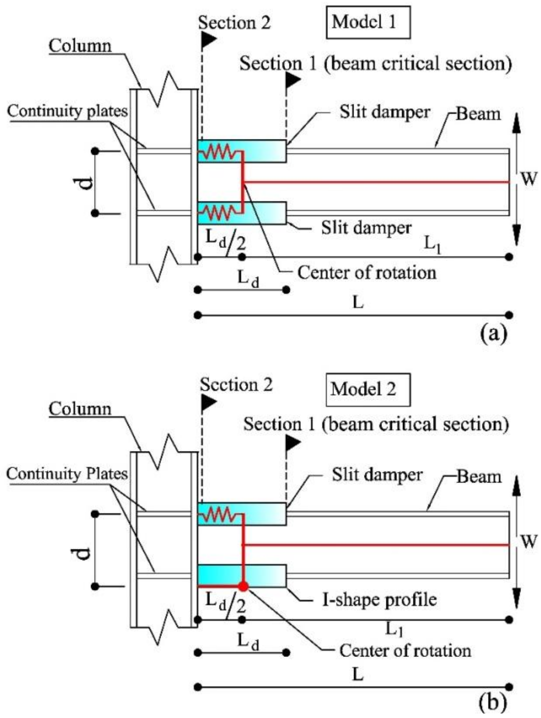

Fig. 4 Analytical models of the slit damper connections: (a) Model 1; (b) Model 2

can be obtained for yield and ultimate state of each model.

If P_y governs on each row of the slit dampers, the shear force in the beam section (W_y) and the maximum bending moment of the connection (M_y) in this case can be obtained as follows

$$W_y = \frac{2P_y.d}{L_1} \tag{4}$$

$$M_y = W_y.L = \frac{2P_y.d.L}{L_1} \tag{5}$$

Where L is the beam length and L_1 is the distance between loading point and middle of the slit dampers.

In model 1, d is the height of beam (Fig. 4(a)) and in model 2, d is the distance between the web of upper damper and the center of rotation.

In the ultimate state, when P_u governs on each row of the slit dampers, beam shear force (W_u) and the maximum bending moment of the connection (M_u) can be obtained as follows

$$W_u = \frac{2P_u.d}{L_1} \tag{6}$$

$$M_u = W_u.L = \frac{2P_u.d.L}{L_1} \tag{7}$$

The yield deformation of slit dampers are analytically calculated (Oh *et al*. 2009) by using elastic equations as follows

$$\Delta_y = \frac{1.5P_y.H_T}{n.E.T.B}\left[(\frac{H'}{B})^2 + 2.6\right] \tag{8}$$

Where E is the modulus of elasticity. The yield deformation of the slit damper can be used to calculate the initial stiffness of connections.

The initial stiffness of the beam to column connection in model 1 and 2 can be estimated as below

$$K^{-1} = K_s^{-1} + K_b^{-1} \tag{9}$$

Where K is the initial stiffness that relates the beam tip displacement under a vertical force. K_s is the slit damper stiffness. K_b is bending stiffness of the beam that it can be calculated as below

$$K_b = \frac{3E.I}{L^3} \tag{10}$$

The term of stiffness that related to the slit dampers (K_s) can be calculated by dividing beam tip force by deflection of the beam tip which is originated from slit dampers deformation. Based on the principle of conservative energy and geometrical relations, the amount of K_s for model 1 and 2 can be obtained as follows:

For model 1:

$$K_s = \frac{W_y}{2\Delta_y(\frac{L_1}{d})} = \frac{W_y.d}{2\Delta_y.L_1} = \frac{P_y}{\Delta_y}\left(\frac{d}{L_1}\right)^2 \tag{11}$$

And for model 2:

$$K_s = \frac{W_y}{\Delta_y(\frac{L_1}{d})} = \frac{W_y.d}{\Delta_y.L_1} = \frac{2P_y}{\Delta_y}\left(\frac{d}{L_1}\right)^2 \tag{12}$$

The specimens are designed to provide the weak-beam and strong-column theory. In this design method, the beam and the slit damper connection have lower moment capacity than the column. This method guarantees that the column remains safe in the elastic state.

In the connection with slit damper, the capacity of the slit damper is governed. In these connections, the geometry of damper is designed in such a way that damper yields before the beam. The critical section of the beam is shown in Fig. 4 (section 1). This section is in the vicinity of the slit dampers.

The maximum bending moment of connection transfers from the slit dampers (section 2) to the column. As it is seen in Fig. 4, the moment in section 2 is greater than the section 1. In other words, the moment capacity of the connection is greater than the bending moment in the critical section of the beam. In this study, slit dampers yield before the beam.

This research is just a case study and elements are designed based on the capacity rules. For example, the length of the holes in the damper is designed to provide sufficient length for fillet welding (Fig. 2). In this length, couple forces transfer from beam flanges to the slit dampers by welding.

Some recommended design rules for other types of dampers were extended by Vasdravellis *et al*. (2014). According to their research for optimum results, the smaller cross-section in the mid-length of the damper piers must be used. They proposed the shape of the pier followed the profile shape of the bending moment diagram as it is shown in Fig. 3(a) (i.e., is minimum at the mid-length of the pier and maximum at the pier ends). In this state, plastic deformations along the piers are distributed uniformly. This optimum design increases energy dissipation, ductility, deformation and delay fracture in the slit damper piers. In this strategy, if the pier end width remains constant and mid-length width decreases, the stiffness of the slit damper connection will be reduced.

4. Experimental setup and connection specimens

In this study, two specimens of slit damper connections were made (Fig. 5). The specimens were half scale. Lengths and sections of the beams and columns were identical in two specimens. In each specimen, the column was made of I-shape steel plate girder and IPE140 profile was used for the beam.

The main differences of two specimens were numbers of the slit dampers. Also, the size and arrangement of slits were different. IPE200 Profiles were used for all slit dampers.

In specimen SDC1, just one slit damper was used at the top of the beam and was connected to the column. In this specimen, an IPE200 profile without any slit connected the bottom flange of the beam to the column. In SDC2, two

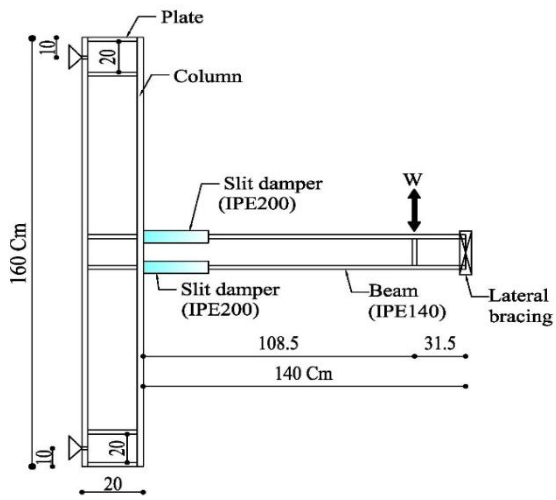

(a) Geometry of connections

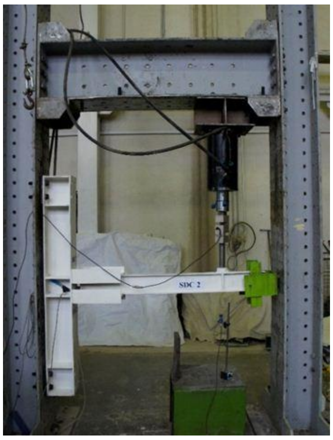

(b) Illustration of specimen SDC2

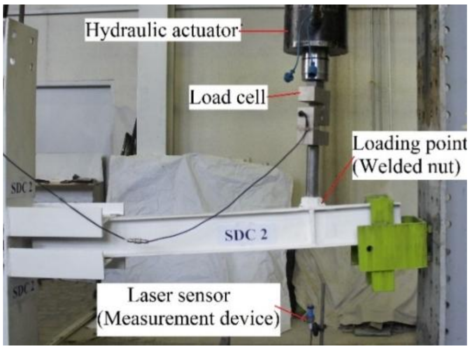

(c) Measurement device and the connection between the loading point and the beam

Fig. 5 Slit damper connection specimen

identical dampers connected the beam flanges to the column.

Weak-beam and strong-column theory is governed on specimens design. Groove welding was used to connect the slit damper to the column face. All fillet welding visually were checked. Also, the ultrasonic test was used to check groove welding. Details of SDC1 and SDC2 are shown in Figs. 6-7.

In the columns, the thickness of flanges, webs and stiffener plates were 10 mm. In each specimen, lateral

Table 1 Mechanical properties of steel materials

Parts of specimen	Thickness (mm)	σ_y (MPa)	σ_u (MPa)	Elongation at fracture (%)
Beam (IPE140)	Web = 4.7	315	483	37.8
	Flange = 6.9	301	464	38.2
Slit damper (IPE200)	Web = 5.6	413	510	29.4
	Flange = 8.5	404	502	31
Column	10	270	420	30

Table 2 Design specifications of specimens

Specimen	W_y (kN)	M_y (kN.m)	W_u (kN)	M_u (kN.m)
SDC1	20.51	22.25	25.33	27.48
SDC2	38.23	41.48	47.20	51.22

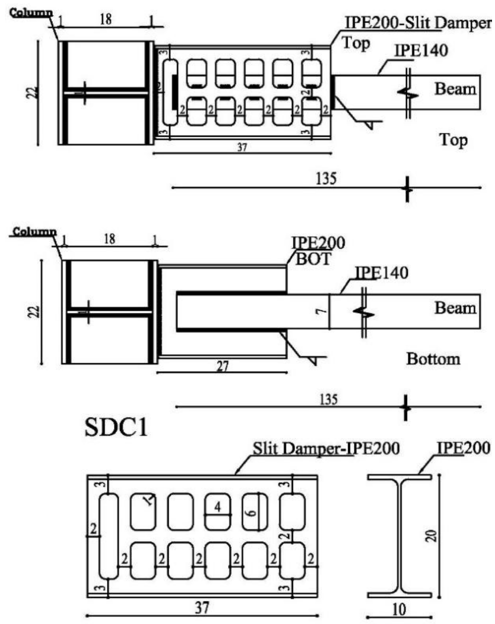

Fig. 6 Details of specimen SDC1

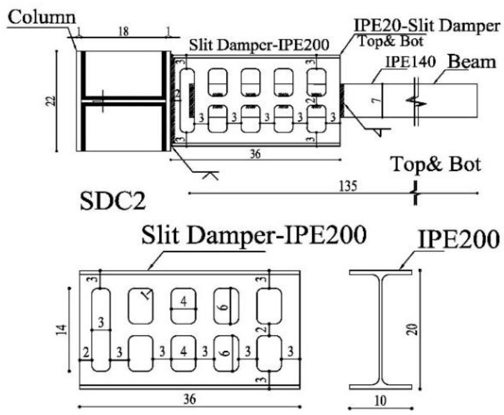

Fig. 7 Details of specimen SDC2

bracing at the end of the beam was used. This bracing prevented lateral buckling of the specimen. All beams were cut from one IPE140 profile. Also, all slit dampers were made of one IPE200 profile.

Mechanical properties of the beams (IPE140), the slit dampers (IPE200) and the columns plates are presented in Table 1. Elongations in Table 1 refer to the point of fracture. Coupons were prepared according to ASTM E8/E8M-16a standard and tested. Stress-strain curve of IPE200 web (damper) is shown in Fig. 8.

Slits of dampers were created by waterjet technology. This technology remains no extra stresses in the materials. Design specifications of specimens are presented in Table 2.

Each specimen was connected to a rigid frame. Hinged supports were used for columns.

Cyclic loading was applied on specimens. The cyclic displacements conditions were continued until 0.06 story drift. Cyclic displacements were applied according to the AISC 341-05 (2005). Displacements of cyclic loading are shown in Fig. 9. Displacements were applied on the beam by a hydraulic actuator which had 250 kN loading capacity (Fig. 5). Loading point was connected to the beam by a welded nut in each specimen. This detail could apply reversible loading on the specimens.

Connection rotations were measured according to FEMA350 criteria (Fig. 10). A laser sensor was used to measure the displacement of the beam beneath the loading point (Fig. 5(c)). Displacements and applied loads were measured during experiments time.

Connection bending moment could be calculated by multiplying applied load by the distance between the loading point and the column side (L = 1.085 m).

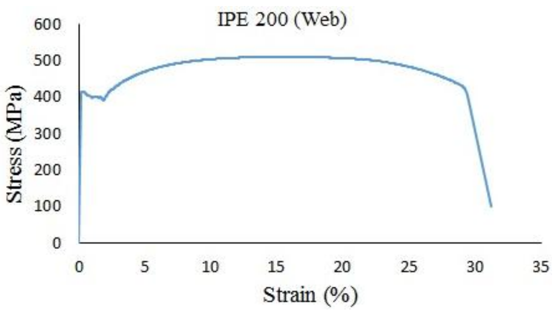

Fig. 8 Stress-strain curve of the slit damper web (standard tension test)

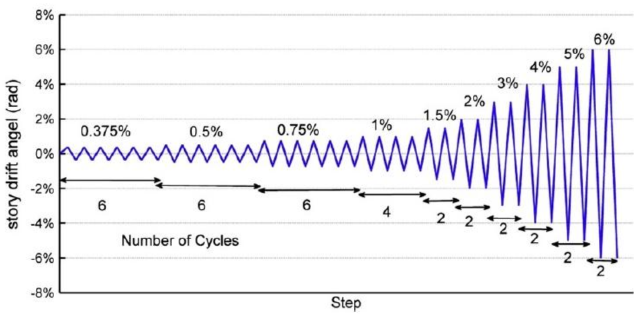

Fig. 9 Displacements of cyclic loading (AISC 341-05)

5. Test observations of specimen SDC1

In this specimen, the beam was connected to the column by a slit damper and one IPE200 profile without any slit. The slit damper connected the top flange of the beam to the column and the bottom flange of the beam was connected to the column by IPE200 Profile. Cyclic loading simulated seismic loading on the connection.

In the first cycle of 0.03 radian rotation, the moment of connection was $1.4M_p$ and some cracks were formed on the struts of the damper. Fracture of the damper is initiated in this stage. Bending moment in the critical section of the beam was lower than M_p for this loading. In the next cycle, cracks were extended. Until the first cycle of 3% drift, bending moment and loading were increased according to increasing of displacements but when drift increased from 3% to 4%, bending moment decreased because of extended cracks on the damper.

In the first cycle of 4% drift, the moment of the connection was equal to $0.95M_p$. This moment is greater than $0.8M_p$ that is recommended by AISC for special moment frames. In the next cycle, the length and width of

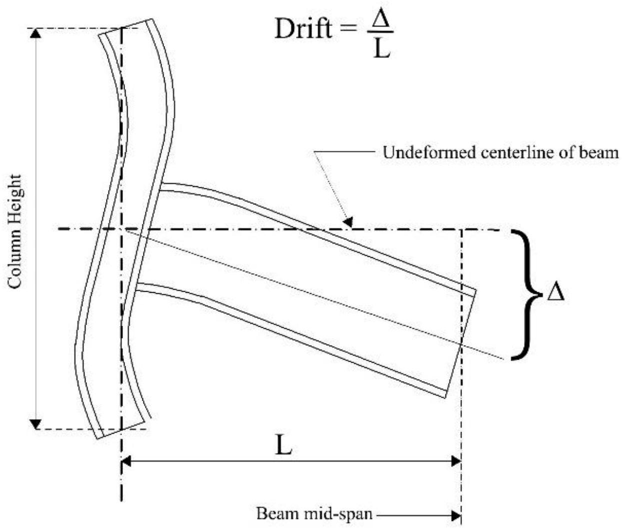

Fig. 10 Story drift (FEMA 350)

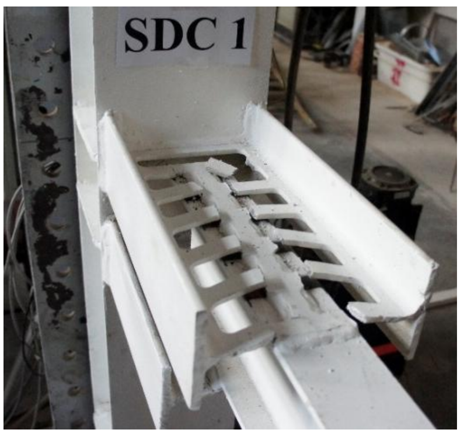

Fig. 11 Specimen SDC1 at the end of the loading process

cracks were extended more. Loading was continued until 6% drift and in this rotation, all struts of damper were cracked completely (Fig. 11).

No cracks or failures were observed on the welding during the whole of the loading process. The observations indicated that the slit damper dissipated energy and prevented damages and failure on the welding. Also, no local buckling was observed on the web or the beam flanges during the loading. At the end of the test, no persistent plastic deformations remained in the column and the panel zone. These matters are the goals of the slit damper design. At the end of the specimen test, all damages occurred in slit damper and other parts of connection remained safe. The observations proved the efficiency of the slit damper connection.

At the end of the test, the beam was still supported by the lower IPE profile. welds between the beam and this profile were without any damages and connection acted as a pin connection.

6. Test observations of specimen SDC2

In this connection, two slit dampers were used to connect the beam to the column. Cyclic displacement loading was applied to the specimen. First cracks on the slit dampers were observed at 4% drift. No decrease in the moment was observed until 4% story drift.

In the first cycle of 4% story drift, connection moment was 1.73M_p. Fracture of the damper is initiated in this stage. Bending moment in the critical section of the beam was about M_p for this loading. The moment of connection decreased to 1.63M_p in the next cycle of 4% story drift. This moment is so greater than 0.8M_p that is recommended by AISC. The increase of story drift to 5% caused that cracks were developed and the moment capacity of connection was decreased. In the first cycle of 5% story drift, the moment of connection was equal to 1.43M_p and in the next cycle, the moment was decreased to 1.09M_p.

The main point is that the first cracks were propagated on the upper and lower dampers and subsequently just cracks on the upper damper were developed. Cracks on the upper damper were extended quickly and stress concentration on it was raised. Thus, cracks on the upper damper were extended more. This damper dissipated more energy. At the end of the test, just primary cracks existed on the struts of the lower damper and the upper damper experienced failure. At the end of the loading process, the lower slit damper supported the beam as a pin support and the specimen remained stable.

In the specimen, no cracks or failure were observed on the welding. Slit dampers dissipated energy and prevented plastic damages on the welding. Also, no local buckling was observed in the web or flanges of the beam. All notes were mentioned above showed the performance of the connection. Specimen SDC1 experienced the reduction of bending moment after 3% story drift because cracks were formed and extended. In the specimen SDC2, this reduction occurred later and after 4% story drift. The reason of the phenomenon is that two dampers were used and less stress concentration occurred in SDC2.

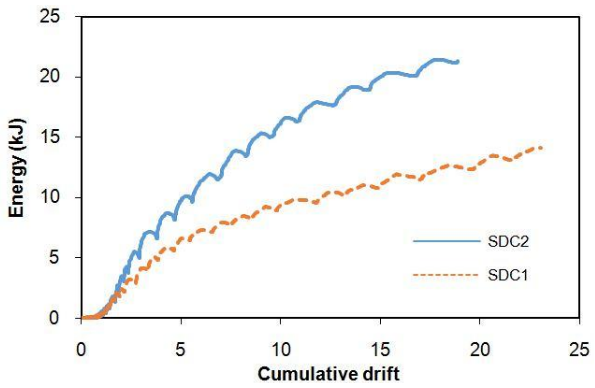

Fig. 12 The cumulative dissipated energy of specimens

The flexibility of specimen SDC2 was more than SDC1. Moment reduction of SDC1 in the first cycle of 4% drift relative to 3% drift was equal to 32%. This value of SDC2 in the first cycle of 5% drift relative to 4% drift was 19%.

7. Energy absorption of specimens

The area under the force-displacement curves of specimens indicates the absorbed energy. Dissipation energy of the specimen SDC1 and SDC2 are equal to 14.13 kJ and 21.39 kJ, respectively. Specimen SDC2 absorbed more energy and showed better performance than SDC1. Specimen SDC2 which had two slit dampers absorbed more energy than SDC1 which had just one slit damper. Structures under the effects of cyclic loads absorb some of the energy as plastic deformations. Value of energy dissipation is an essential parameter for ductile structures. Energy is equal to force multiply by its displacement. Energy dissipation is equal to the area under the load vs. displacement curves in hysteresis diagrams. Dissipated energy graphs of experimental specimens are shown in Fig. 12. Structures which absorb more energy have more efficiency in the cyclic loads such as an earthquake. This parameter expressed ductility of the structure. As it is shown in Fig. 12, SDC2 absorbed about 51% more energy than SDC1.

8. Finite element models

Numerical models of the connection specimens were made and the results of these models compared with the experimental data. The models were investigated under cyclic loading similar to test conditions. The models were made by ABAQUS software. Shell elements S4R were used to model structural parts such as beams, columns, and dampers. S4R is a shell element which has 4 nodes. Each node of the element has 6 degrees of freedom. Mechanical properties of the steel materials were defined according to the results of materials test. According to the results of the coupon tensile test, a true stress-strain curve with reduced strength at large strain after the ultimate strain was defined. The strength of materials which experience strains more than the ultimate strain is decreased to simulate the behavior of the materials. In the numerical models, cracks on the dampers were not modeled. This method was used by many researchers such as Pachoumis *et al*. (2010) and Faridmehr *et al*. (2015). They simulated connections for the large deformations. This method could simulate moment reduction in the last cycles. Stress-strain curve for the web of IPE200 (damper) according to ASTM standard test is shown in Fig. 8. Lateral bracing conditions were introduced similar to the experimental conditions. In the experimental study, buckling of the elements did not observe so buckling analysis and initial imperfections did not consider in the numerical models.

The potential for yielding and failure was evaluated based on tendency of Von Mises stress and equivalent plastic strain (PEEQ). PEEQ is a scalar quantity of the accumulated plastic strains. In reversal loadings, if the plastic strain rate is non-zero (regardless of plastic strain sign), PEEQ continues to increase. Von Mises stress contours of models SDC1 and SDC2 at 3% and 4% story drift are respectively is shown in Fig. 13. PEEQ contours are plotted in Fig. 14. As it is seen in the PEEQ contours, the most plastic strains and deformations occurred in the dampers and other parts remained safe.

The Von Mises stress and PEEQ criterions have used to determine yielding and failure points of the metal materials in a complex stress state. In Von Mises and PEEQ contours, the points of stress concentrations are exactly placed on the cracked struts of experimental specimens.

Hysteretic and skeleton curves of experimental specimens and numerical models are shown in Figs. 15-16. Skeleton curve indicates maximum bending moments of each loading cycle vs. rotations. Numerical hysteretic and skeleton curves have good agreement with the experimental curves. One RBS connection was modeled by ABAQUS and results were compared with the experimental specimens data. Specifications of RBS connection model was similar to the experimental specimens. In the RBS model, reduction shape of flanges was a circular segment. Skeleton curves of the RBS connection model and experimental specimens are shown in Fig. 16. As it is seen in Fig. 16, SDC1 had the most initial stiffness. SDC2 and RBS models had equal initial stiffness approximately. Skeleton curves of 3 types of connections are completely different at 2.5% drift. SDC1

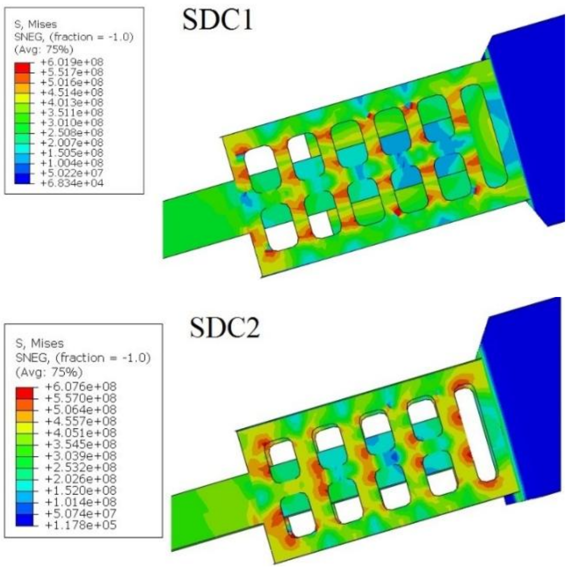

Fig. 13 Von Mises contours of models

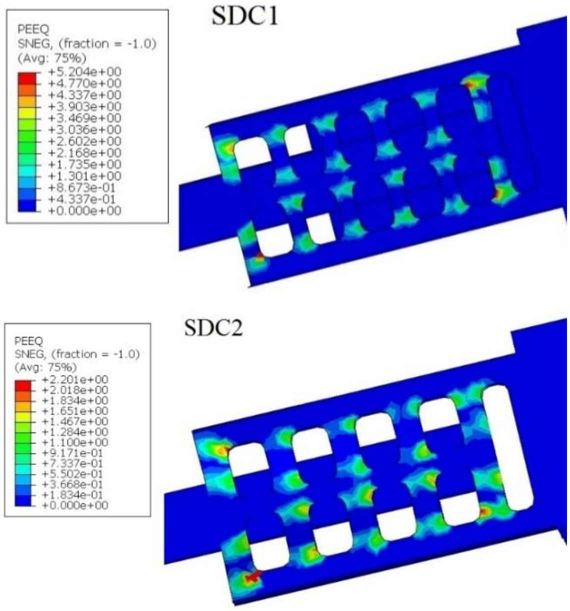

Fig. 14 PEEQ contours of models

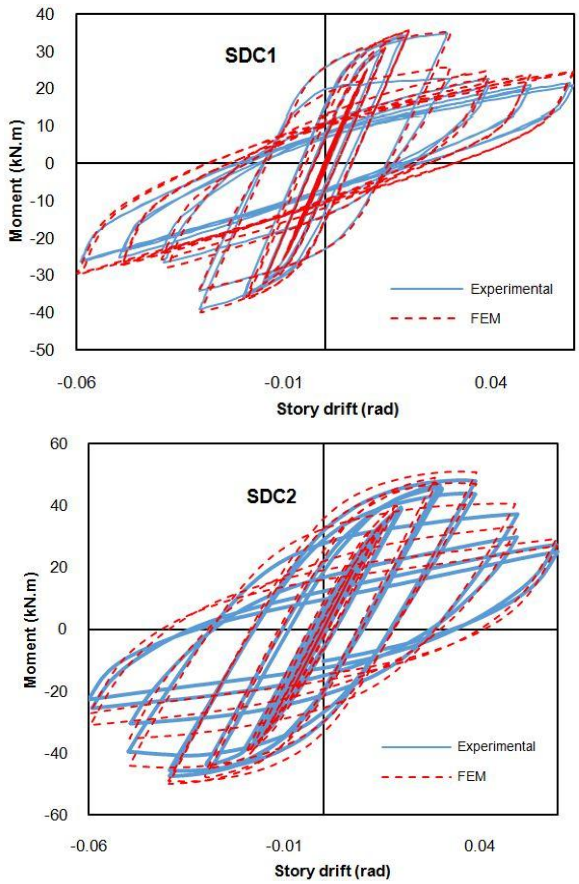

Fig. 15 Comparison of hysteretic moment-rotation curves of experimental specimens with numerical models

experienced moment reduction after 3% drift. SDC2 and RBS models experienced moment reduction after 4% drift. SDC2 had the most moment capacity and experienced $1.73M_p$. The most moment of SDC1 and RBS model were $1.4M_p$ and $1.28M_p$, respectively. The results of theoretical relations, numerical analysis, and experimental data are presented in Table 3. As it was presented in Table 3, the numerical and experimental results for both specimens are close together. Theoretical results which are obtained from model 1 predict the results of specimen SDC2 close to the experimental and numerical data. Analytical model 1 predicts a lower bending moment for specimen SDC1.As it was expressed before (Sec. 3), the reason for this matter is differences between stiffness and structural properties of the upper and lower I-shape profiles (springs) in SDC1

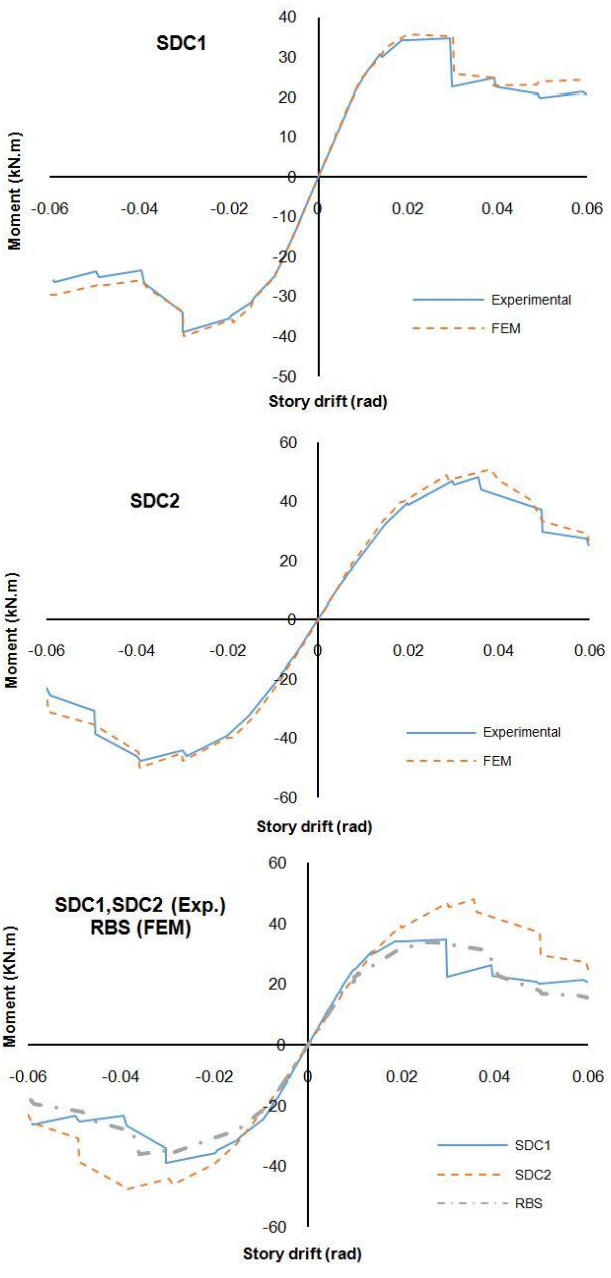

Fig. 16 Comparison between moment-rotation skeleton curves of experimental specimens and FEM

Table 3 Maximum bending moment of the connections

	Model	M_u (kN.m) Theoretical	M_u (kN.m) FEM	M_u (kN.m) Experimental
SDC1	Model 1	27.48	39.93	38.99
	Model 2	37.29		
SDC2	Model 1	51.22	50.84	48.16

Table 4 Connection stiffness

Model	Theoretical N/mm	FEM N/mm	Experimental N/mm
SDC1	2302	2059	2050
SDC2	2080	1931	1790

specimen. According to the results, this simplified model is not accurate for specimen SDC1. So model 2 was used to predict the bending moment for specimen SDC1.

As it is observed, the results of model 2 are close to the experimental and numerical results. Based on the theoretical relations, numerical analysis, and experimental data, initial stiffnesses of two specimens are calculated and presented in Table 4. Model 1 was used to calculate the theoretical stiffness of SDC2 and model 2 was used for SDC1. As it was seen in Table 4, the numerical and experimental results for initial stiffness are close together. The theoretical initial stiffnesses of specimens are greater than experimental and numerical stiffnesses. The reason of this matter is that in theoretical models, deformations of panel zone and column have not considered while experimental and numerical results contain these deformations. Panel zone stiffness could be considered by using the method provided by Eurocode 3 part 1-8 (2004). In this study, the panel zone is stiffened by continuity plates. In this case, the method proposes an infinite amount for panel zone stiffness. This method will not have a significant influence on the results.

9. Conclusions

In this study, two new beam to column connections with the slit dampers were introduced. Just one slit damper was used in specimen SDC1 and other detail (SDC2) had two slit dampers. According to the test results, proposed connections were shown high performance under cyclic loading. No cracks were observed in the dampers until 3% story drift.

In specimen SDC1, the maximum bending moment at 3% story drift was $1.4M_p$ and moment of connection at 4% story drift was $0.95M_p$. In specimen SDC2, the most bending moment at 4% story drift was $1.73M_p$. Both proposed connections have moment capacity more than $0.8M_p$ that was recommended by AISC. Specimen SDC2 which has two slit dampers is more ductile. Energy absorption and moment capacity of SDC2 are more than specimen SDC1.

Proposed connections provide Plastic rotation capacity according to seismic design codes criteria. Bending moment capacity of the connections is greater than the recommended value of mentioned codes. Based on the experimental results, the followings are concluded:

- Damages of welding are prevalent in common connections but proposed connections prevent welding damages and stress concentration in the welding. In both specimens, no cracks and damages were observed in the welding.
- During the loading process, plastic deformations were formed in the slit dampers. In other words, all energy was dissipated by slit dampers approximately. Other parts of connections remain safe and no damages occurred.
- During the loading process, no local buckling of beam web or flanges was observed.
- The energy absorption capacity of specimen SDC2 which had two slit dampers is more than SDC1. Energy absorption ratio of SDC2 to SDC1 is 1.51 and the maximum bending moment ratio of SDC2 to SDC1 is 1.23.

Two main aims are followed by using dampers: prevention of damages in the beam, column, welding, and panel zone and also increase of the beam to column connection ductility. According to the mentioned items above, all these goals are fulfilled by the experimental results. In other words, the proposed connections provide specifications of seismic design codes. Further studies and researches are required to recognize the behavior of proposed connections.

References

AISC 341-10 (2010), Seismic Provisions for Structural Steel Buildings; American Institute of Steel Construction, Chicago, IL, USA.

AISC 358-10 (2010), Prequalified connections for special and intermediate steel moment frames for seismic applications; American Institute of Steel Construction, Chicago, IL, USA.

Amiri, H.A., Najafabadi, E.P. and Estekanchi, H.E. (2018), "Experimental and analytical study of Block Slit Damper", *J. Constr. Steel Res.*, **141**, 167-178. https://doi.org/10.1016/j.jcsr.2017.11.006

ASTM E8/E8M-16a (2016), Standard test methods for tension testing of metallic materials; American Society for Testing Materials, PA, USA.

Benavent-Climent, A. (2010), "A brace-type seismic damper based on yielding the walls of hollow structural sections", *Eng. Struct.*, **32**(4), 1113-1122. https://doi.org/10.1016/j.engstruct.2009.12.037

Chan, R.W. and Albermani, F. (2008), "Experimental study of steel slit damper for passive energy dissipation", *Eng. Struct.*, **30**(4), 1058-1066. https://doi.org/10.1016/j.engstruct.2007.07.005

Eldin, M.N., Kim, J. and Kim, J. (2018), "Optimum distribution of steel slit-friction hybrid dampers based on life cycle cost", *Steel Compos. Struct., Int. J.*, **27**(5), 633-646. http://dx.doi.org/10.12989/scs.2018.27.5.633

Eurocode 3 (2004), Design of steel structures - Part 1-8: Design of Joints, Brussels, Belium.

Faridmehr, I., Osman, M.H., Tahir, M.M., Nejad, A.F. and Hodjati, R. (2015), "Severe loading assessment of modern and new proposed beam to column connections", *Lat. Am. J. Solids Struct.*, **12**(7), 1202-1223. http://dx.doi.org/10.1590/1679-78251286

Farrokhi, H., Danesh, F.A. and Eshghi, S. (2010), "The structural detailing effect on seismic behavior of steel moment resisting connections", *Struct. Eng. Mech., Int. J.*, **35**(5), 617-630. http://dx.doi.org/10.12989/sem.2010.35.5.617

FEMA-350 (2000), Recommended seismic design criteria for new steel moment-frame buildings; Federal Emergency Management Agency, Washington DC, USA.

FEMA-355D (2000), State of the art report on connection performance; Federal Emergency Management Agency, Washington DC, USA.

He, L., Togo, T., Hayashi, K., Kurata, M. and Nakashima, M. (2016), "Cyclic behavior of multirow slit shear walls made from low-yield-point steel", *J. Struct. Eng.*, **142**(11), 04016094. https://doi.org/10.1061/(ASCE)ST.1943-541X.0001569

Hedayat, A.A. (2015), "Prediction of the force displacement capacity boundary of an unbuckled steel slit damper", *J. Constr. Steel Res.*, **114**, 30-50. https://doi.org/10.1016/j.jcsr.2015.07.003

Ibrahim, R. (2008), "Recent advances in nonlinear passive vibration isolators", *J. Sound Vib.*, **314**(3-5), 371-452. https://doi.org/10.1016/j.jsv.2008.01.014

Jones, S.L., Fry, G.T. and Engelhardt, M.D. (2002), "Experimental evaluation of cyclically loaded reduced beam section moment connections", *J. Struct. Eng.*, **128**(4), 441-451. https://doi.org/10.1061/(ASCE)0733-9445(2002)128:4(441)

Karamodin, A. and Zanganeh, A. (2017), "Seismic Design and Performance of Dual Moment and Eccentrically Braced Frame System Using PBPD Method", *Lat. Am. J. Solids Struct.*, **14**(3), 441-463. http://dx.doi.org/10.1590/1679-78253425

Karavasilis, T.L., Kerawala, S. and Hale, E. (2012), "Hysteretic model for steel energy dissipation devices and evaluation of a minimal-damage seismic design approach for steel buildings", *J. Constr. Steel Res.*, **70**, 358-367. https://doi.org/10.1016/j.jcsr.2011.10.010

Ke, K. and Chen, Y. (2014), "Energy-based damage-control design of steel frames with steel slit walls", *Struct. Eng. Mech., Int. J.*, **52**(6), 1157-1176. http://dx.doi.org/10.12989/sem.2014.52.6.1157

Khatamirad, M. and Shariatmadar, H. (2017), "Experimental and analytical study of steel slit shear wall", *Steel Compos. Struct., Int. J.*, **24**(6), 741-751. http://dx.doi.org/10.12989/scs.2017.24.6.741

Kim, J., Kim, M. and Eldin, M.N. (2017), "Optimal distribution of steel plate slit dampers for seismic retrofit of structures", *Steel Compos. Struct., Int. J.*, **25**(4), 473-484. http://dx.doi.org/10.12989/scs.2017.25.4.473

Lee, J. and Kim, J. (2015), "Seismic performance evaluation of moment frames with slit-friction hybrid dampers", *Earthq. Struct., Int. J.*, **9**(6), 1291-1311. http://dx.doi.org/10.12989/eas.2015.9.6.1291

Li, B., Yang, Q. and Yang, N. (2011), "An investigation on aseismic connection with opening in beam web in steel moment frames", *Adv. Struct. Eng.*, **14**(3), 575-587. https://doi.org/10.1260/1369-4332.14.3.575

Lu, J., Qiao, X., Liao, J. and Tang, Y. (2016), "Experimental study and numerical simulation on steel plate shear walls with non-uniform spacing slits", *Int. J. Steel Struct.*, **16**(4), 1373-1380. https://doi.org/10.1007/s13296-016-0044-5

Mahjoubi, S. and Maleki, S. (2016), "Seismic performance evaluation and design of steel structures equipped with dual-pipe dampers", *J. Constr. Steel Res.*, **122**, 25-39. https://doi.org/10.1016/j.jcsr.2016.01.023

Mirghaderi, S.R., Torabian, S. and Imanpour, A. (2010), "Seismic performance of the Accordion-Web RBS connection", *J. Constr. Steel Res*, **66**(2), 277-288. https://doi.org/10.1016/j.jcsr.2009.09.007

Oh, S.-H., Kim, Y.-J. and Ryu, H.-S. (2009), "Seismic performance of steel structures with slit dampers", *Eng. Struct.*, **31**(9), 1997-2008. https://doi.org/10.1016/j.engstruct.2009.03.003

Pachoumis, D.T., Galoussis, E.G., Kalfas, C.N. and Efthimiou, I.Z. (2010), "Cyclic performance of steel moment-resisting connections with reduced beam sections—experimental analysis and finite element model simulation", *Eng. Struct.*, **32**(9), 2683-2692. https://doi.org/10.1016/j.engstruct.2010.04.038

Popov, E.P. and Tsai, K.-C. (1989), "Performance of large seismic steel moment connections under cyclic loads", *Eng. J.*, **26**(2), 51-60.

Saffari, H., Hedayat, A. and Nejad, M.P. (2013), "Post-Northridge connections with slit dampers to enhance strength and ductility", *J. Constr. Steel Res.*, **80**, 138-152. https://doi.org/10.1016/j.jcsr.2012.09.023

Saleh, A., Zahrai, S.M. and Mirghaderi, S.R. (2016), "Experimental study on innovative tubular web RBS connections in steel MRFs with typical shallow beams", *Struct. Eng. Mech., Int. J.*, **57**(5), 785-808. http://dx.doi.org/10.12989/sem.2016.57.5.785

Shahri, S.F. and Mousavi, S.R. (2018), "Seismic behavior of beam-to-column connections with elliptic slit dampers", *Steel Compos. Struct., Int. J.*, **26**(3), 289-301. http://dx.doi.org/10.12989/scs.2018.26.3.289

Tabar, A.M. and Deylami, A. (2006), "Investigation of major parameters affecting instablility of steel beams with RBS moment connections", *Steel Compos. Struct., Int. J.*, **6**(3), 203-219. http://dx.doi.org/10.12989/scs.2006.6.3.203

Tagawa, H., Yamanishi, T., Takaki, A. and Chan, R.W. (2016), "Cyclic behavior of seesaw energy dissipation system with steel slit dampers", *J. Constr. Steel Res.*, **117**, 24-34. https://doi.org/10.1016/j.jcsr.2015.09.014

Vasdravellis, G., Karavasilis, T.L. and Uy, B. (2012), "Large-scale experimental validation of steel posttensioned connections with web hourglass pins", *J. Struct. Eng.*, **139**(6), 1033-1042. https://doi.org/10.1061/(ASCE)ST.1943-541X.0000696

Vasdravellis, G., Karavasilis, T.L. and Uy, B. (2014), "Design rules, experimental evaluation, and fracture models for high-strength and stainless-steel hourglass shape energy dissipation devices", *J. Struct. Eng.*, **140**(11), 04014087. https://doi.org/10.1061/(ASCE)ST.1943-541X.0001014

Zahrai, S.M., Mirghaderi, S.R. and Saleh, A. (2017), "Tubular Web Reduced Beam Section (TW-RBS) connection, a numerical and experimental study and result comparison", *Steel Compos. Struct., Int. J.*, **23**(5), 571-583. http://dx.doi.org/10.12989/scs.2017.23.5.571

Zheng, J., Li, A. and Guo, T. (2015), "Analytical and experimental study on mild steel dampers with non-uniform vertical slits", *Earthq. Eng. Eng. Vib.*, **14**(1), 111-123. https://doi.org/10.1007/s11803-015-0010-9

Zhou, Q. and Lu, X. (2004), "Shaking table test and numerical analysis of a combined energy dissipation system with metallic yield dampers and oil dampers", *Struct. Eng. Mech., Int. J.*, **17**(2), 187-201. http://dx.doi.org/10.12989/sem.2004.17.2.187

BU